Short-lived chlorine-36 in a Ca- and Al-rich inclusion from the Ningqiang carbonaceous chondrite

Yangting Lin[†‡§], Yunbin Guan[‡], Laurie A. Leshin[‡¶], Ziyuan Ouyang[‖], and Daode Wang[††]

[†]State Key Laboratory of Lithosphere Tectonic Evolution, Institute of Geology and Geophysics, Chinese Academy of Sciences, Beijing 100029, China; [‡]Department of Geological Sciences and [¶]Center for Meteorite Studies, Arizona State University, Tempe, AZ 85287-1404; [‖]National Astronomy Observatory, Chinese Academy of Sciences, Beijing 100012, China; and [††]Guangzhou Institute of Geochemistry, Chinese Academy of Sciences, Guangzhou 510640, China

Communicated by Ho-kwang Mao, Carnegie Institution of Washington, Washington, DC, September 29, 2004 (received for review August 17, 2004)

Excesses of sulfur-36 in sodalite, a chlorine-rich mineral, in a calcium- and aluminum-rich inclusion from the Ningqiang carbonaceous chondrite linearly correlate with chorine/sulfur ratios, providing direct evidence for the presence of short-lived chlorine-36 (with a half-life of 0.3 million years) in the early solar system. The best inferred $(^{36}Cl/^{35}Cl)_o$ ratios of the sodalite are $\approx 5 \times 10^{-6}$. Different from other short-lived radionuclides, chlorine-36 was introduced into the inclusion by solid-gas reaction during secondary alteration. The alteration reaction probably took place at least 1.5 million years after the first formation of the inclusion, based on the correlated study of the ^{26}Al-^{26}Mg systems of the relict primary minerals and the alteration assemblages, from which we inferred an initial ratio of $(^{36}Cl/^{35}Cl)_o \geq 1.6 \times 10^{-4}$ at the time when calcium- and aluminum-rich inclusions formed. This discovery supports a supernova origin of short-lived nuclides [Cameron, A. G. W., Hoeflich, P., Myers, P. C. & Clayton, D. D. (1995) *Astrophys. J.* 447, L53; Wasserburg, G. J., Gallino, R. & Busso, M. (1998) *Astrophys. J.* 500, L189–L193], but presents a serious challenge for local irradiation models [Shu, F. H., Shang, H., Glassgold, A. E. & Lee, T. (1997) *Science* 277, 1475–1479; Gounelle, M., Shu, F. H., Shang, H., Glassgold, A. E., Rehm, K. E. & Lee, T. (2001) *Astrophys. J.* 548, 1051–1070]. Furthermore, the short-lived ^{36}Cl may serve as a unique fine-scale chronometer for volatile-rock interaction in the early solar system because of its close association with aqueous and/or anhydrous alteration processes.

meteorite | solar nebula | sulfur isotopes | magnesium isotopes | chronometer

Short-lived, now extinct, radionuclides have been detected in primitive meteorites (1). They have been intensively studied and are still subjects of ongoing great interest for broad scientific audiences, because short-lived radionuclides may serve as the only available fine-scale chronometers to trace processes in the early solar system (1, 2), and their relative abundance can constrain the local galactic environment of solar system formation (3–6). However, the origin of short-lived radionuclides is a long-standing issue. One scenario holds that the short-lived radionuclides originated in stellar sources like supernovae (3, 7) or asymptotic giant branch stars (5, 6) in close proximity to the forming solar system. According to such a stellar origin, short-lived radionuclides were injected homogeneously in the solar nebula, hence they may be used as chronometers. This idea is supported by the measurement of U-Pb absolute ages of Ca- and Al-rich inclusions (CAIs) and chondrules with a ≈1-million year (My) resolution (8), which yields a time interval between formation of CAIs and chondrules similar to that inferred by many ^{26}Al-^{26}Mg measurements, although a recent study reported that chondrule formation began contemporaneously with the formation of CAIs (9). On the other hand, the same short-lived radionuclides may be produced locally by intense irradiation of nebular materials by the proto-sun (10–12). The predictions of local irradiation models (4, 13) are compatible with the observed abundance of some nuclides (e.g., ^{10}Be, ^{26}Al, ^{41}Ca, and ^{53}Mn). According to local irradiation models, the systematically different initial $(^{26}Al/^{27}Al)_o$ ratios between CAIs and chondrules are related to their different distances from the proto-sun, bearing no temporal significance.

Chlorine-36 has a half-life of 0.3 My and decays to either ^{36}Ar (98.1%, β^-) or ^{36}S (1.9%, ε and β^+) (14), hence it can be detected by measuring the excess of ^{36}Ar or ^{36}S. A previous study reported the excess of ^{36}Ar in matrix of the Efremovka carbonaceous chondrite (15), which was attributed to the decay of short-lived ^{36}Cl. In this study, we provide direct evidence for the existence of live ^{36}Cl in primitive meteorites based on excess of ^{36}S and its correlation with Cl/S ratios of the samples. The suitable samples for this purpose are sodalite ($Na_8Al_6Si_6O_{24}Cl_2$) in CAIs, because this mineral is Cl-rich (≈7.5 wt%) and CAIs are the oldest assemblages of the solar system (16, 17).

Methods

Because only 1.9% ^{36}Cl decays to ^{36}S, the excess ^{36}S $[(^{36}S/^{34}S)^*]$ can be calculated in the following relationship:

$$(^{36}S/^{34}S)^* = (^{36}S/^{34}S)_m - (^{36}S/^{34}S)_o = 0.019 \times (^{36}Cl/^{35}Cl)_o/(^{35}Cl/^{34}S), \quad [1]$$

where $(^{36}S/^{34}S)_m$ and $(^{36}S/^{34}S)_o$ are the measured and initial (or normal) S isotopic ratios at the time of closure. The inferred $(^{36}Cl/^{35}Cl)_o$ ratio can be calculated from Eq. **1**.

In secondary ion MS analysis, $(^{36}S/^{34}S)^*$ in a sample is detected by measuring its S isotopes relative to standards. S isotopic data are reported as delta values, defined as:

$$\Delta^{33}S = ((^{33}S/^{34}S)_m/(^{33}S/^{34}S)_s - 1) \times 1{,}000 \quad [2]$$

and

$$\Delta^{36}S = ((^{36}S/^{34}S)_m/(^{36}S/^{34}S)_s - 1) \times 1{,}000, \quad [3]$$

where m indicates measured ratios and s indicates standard's normal S isotope ratios. Because of its high abundance, ^{32}S is not used here as the reference isotope. The fractionation-corrected isotopic anomaly in ^{36}S is then calculated from the linear "law":

$$\delta^{36}S = \Delta^{36}S + 2\Delta^{33}S. \quad [4]$$

Sulfur isotopes (^{33}S, ^{34}S, and ^{36}S) and ^{35}Cl of the samples were analyzed by using the Cameca ims-6f ion microprobe at Arizona State University. A small (<10 μm) Cs^+ primary beam of <0.1 nA at 10 keV size was used. Secondary ions were accelerated to −9 keV and collected with an electron multiplier, and dead-time correction was applied to the data. Transfer lenses were tuned for a 75-μm imaged field to increase the secondary ion transmission. Depending on the phase being analyzed, each measurement ran 30–200 cycles through the mass sequence, ^{33}S, ^{34}S, ^{35}Cl,

Abbreviations: CAI, Ca- and Al-rich inclusion; My, million years.

§To whom correspondence should be addressed. E-mail: linyt@mail.igcas.ac.cn.

www.pnas.org/cgi/doi/10.1073/pnas.0407173101

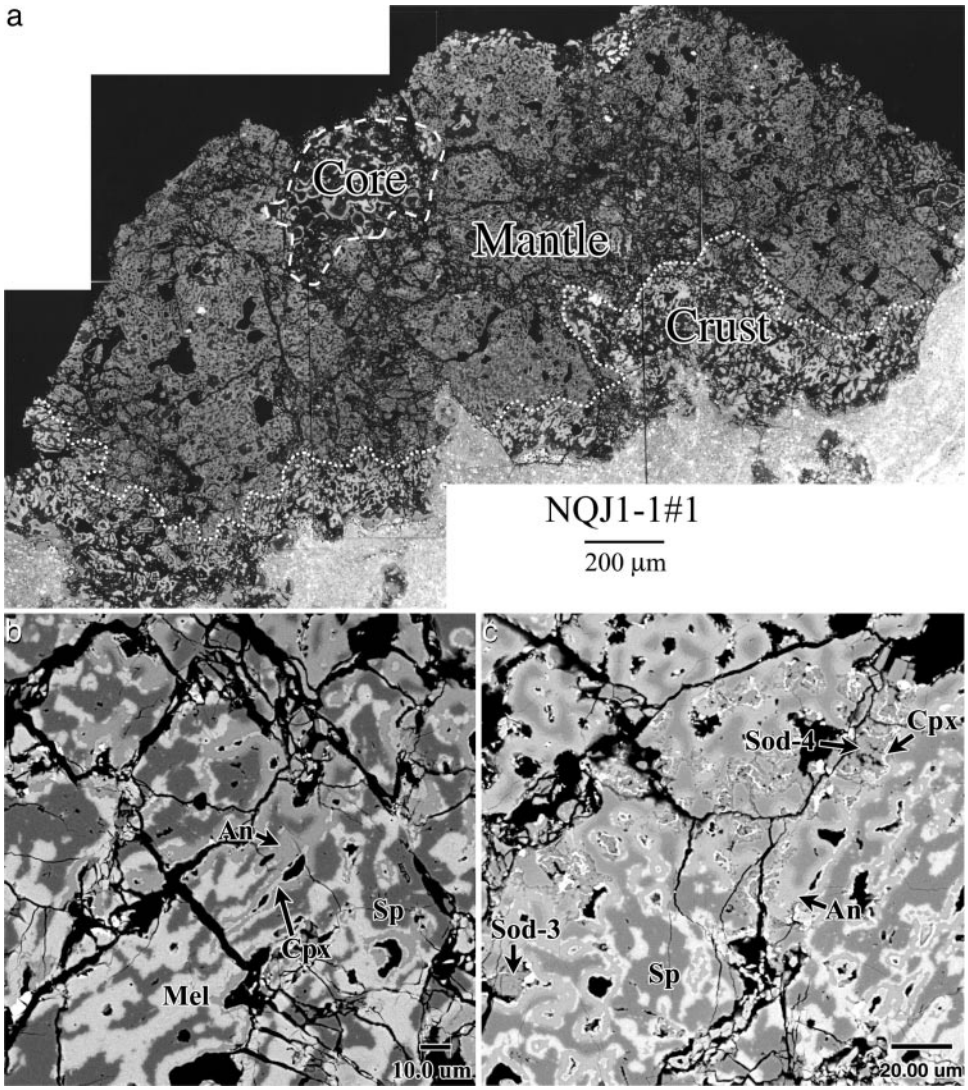

Fig. 1. Back-scattered electron images of the CAI (NQJ1-1#1) from the Ningqiang meteorite. (*a*) The whole CAI shows an annealing texture and consists of a spinel-rich core, a spinel-anorthite-Ca-pyroxene mantle, and a melilite-spinel crust. (*b*) Inset along the crust-mantle boundary, showing replacement of melilite (Mel) by anorthite (An) and Ca-pyroxene (thin light gray rims between dark voids and gray anorthite). The dark gray mineral is spinel (Sp). (*c*) Inset of the mantle, showing anorthite replaced by sodalite-nepheline assemblages (Sod-3 and Sod-4 were analyzed by the ion probe). Thin white rims in the assemblages are Ca-pyroxene (Cpx).

and ^{36}S, with integration times set to 3, 1, 1, and 30 s, respectively. Even with the instrumental conditions set up to allow the highest possible transmission of secondary ions, a long collecting time was still required to achieve reasonable statistical precision because of the low count rates of the S isotopes in sodalite. Hydride and other molecular interferences to the S isotopes were eliminated under high mass resolution conditions with a mass resolving power ($m/\Delta m$) of ≈4,300. Relative to the sulfur isotope standard, Canyon Diablo troilite, troilite (FeS), and djerfisherite $[(K,Na)_6(Fe,Ni,Cu)_{25}S_{26}Cl]$ in the Qingzhen enstatite chondrite should have normal sulfur isotope composition within the precision of the ion microprobe. Therefore, they were used repeatedly as standards to check instrumental mass fractionation (IMF) and verify that no ^{36}S anomaly exists in their measurements. For both standards and samples, IMF was internally corrected by using $^{33}S/^{34}S$ according to the linear law. Because there are no suitable silicate standards, the relative sensitivity factor of $^{35}Cl/^{34}S$ (≈0.6) used throughout this study was determined from djerfisherite in Qingzhen. This may introduce a slight uncertainty in the slopes of the lines, but does not significantly affect the results.

Because sodalite is a secondary phase replacing primary minerals of CAIs during alteration processes, a combined study of ^{26}Al-^{26}Mg systems of individual minerals of the CAI was carried out to determine the time interval between formation and alteration of the CAI. The measurements of magnesium isotopes were carried out by using the same ion microprobe with a −12.5 keV O^- primary beam of <0.4 nA for different mineral phases, including melilite (a solid solution of $Ca_2MgSi_2O_7$-$Ca_2Al_2SiO_7$), plagioclase, and sodalite. Positive secondary ions were accelerated to +9 keV and collected with an energy band-pass of ≈50 eV, an imaged field of ≈75 μm, and a mass resolving power of ≈3,500. The relative sensitivity factors of Al/Mg were determined by using terrestrial standards of melilite and plagioclase.

Results

Three CAIs from the Ningqiang carbonaceous chondrite and two EH3 enstatite chondrites (EET 87746 and ALH 77295) were

GEOPHYSICS

Table 1. Sulfur isotopic compositions and Cl/S ratios

Analysis	$^{35}Cl/^{34}S$, $\pm 2\ \sigma$	$^{36}S/^{34}S \times 10^3$, $\pm 2\ \sigma$
Sod-1a	2,905 ± 217	3.81 ± 0.38
Sod-1b	4,287 ± 210	4.09 ± 0.58
Sod-1c	7,031 ± 385	4.33 ± 0.60
Sod-1d	6,289 ± 435	4.48 ± 0.46
av. Tr-1	<0.01	3.434 ± 0.003
av. Dj-1	0.75 ± 0.01	3.420 ± 0.002
Sod-2a	26,872 ± 2493	5.64 ± 1.15
Sod-2b	10,031 ± 1045	4.84 ± 1.00
Sod-2c	22,942 ± 1475	5.59 ± 0.98
Sod-2d	24,977 ± 1496	5.72 ± 0.94
Sod-2e	38,533 ± 3777	7.37 ± 1.98
Sod-2f	32,931 ± 2936	7.12 ± 1.54
av. Tr-2	<0.01	3.436 ± 0.013
Sod-3a	10,141 ± 637	5.70 ± 0.94
Sod-3b	13,151 ± 800	6.17 ± 0.78
Sod-3c	7,924 ± 447	5.63 ± 0.85
Sod-3d	7,816 ± 332	6.11 ± 0.73
Sod-3e	9,147 ± 426	4.52 ± 0.73
Sod-3f	5,894 ± 372	3.93 ± 0.75
av. Tr-3	<0.01	3.436 ± 0.002
A_sod-1a	18 ± 4	3.57 ± 0.09
Sod-3a	19,958 ± 1,198	6.33 ± 1.19
Sod-3b	36,306 ± 3,490	6.92 ± 1.29
Sod-3c	49,896 ± 2,506	7.36 ± 0.94
Sod-3d	57,486 ± 4,797	7.51 ± 1.59
Sod-3e	52,159 ± 4,215	8.34 ± 1.39
Sod-3f	44,581 ± 3,808	8.39 ± 1.67
av. Tr-3	<0.01	3.431 ± 0.003

Except for one analysis (A_sod-1a) of sodalite (Sod) in ALH 77295, others are in the Ningqiang CAI. Analyses of troilite (Tr) and djerfisherite (Dj) in the Qingzhen enstatite chondrite are given as averages (av.).

studied. The Ningqiang CAI (NQJ1–1#1) has a spinel-rich core, a spinel-anorthite-Ca-pyroxene mantle, and a melilite-spinel crust (Fig. 1*a*). Along the boundaries between the crust and the mantle, anorthite shows a texture of replacing melilite (Fig. 1*b*). In turn, sodalite and much less abundant nepheline occur as alteration products in place of anorthite mainly in the mantle (Fig. 1*c*). The two CAIs from EET 87746 and ALH 77295 are highly altered, consisting of spinel, pyroxene, and fine-grained sodalite and nepheline.

Four sodalite-rich alteration assemblages in the Ningqiang CAI with very high $^{35}Cl/^{34}S$ ratios (up to 57,000) show clear ^{36}S excesses that correlate with $^{35}Cl/^{34}S$ ratios (Table 1 and Fig. 2), suggesting *in situ* decay of ^{36}Cl and excluding possible anomaly of sulfur isotopes or spallogenic ^{36}S. The inferred $(^{36}Cl/^{35}Cl)_o$ ratios are determined from the slopes of the correlation lines in Fig. 2, calibrated for 1.9% decay of ^{36}Cl to ^{36}S. The inferred $(^{36}Cl/^{35}Cl)_o$ ratios ($\pm 2\ \sigma$) are: $(4.6 \pm 0.6) \times 10^{-6}$, $(5.1 \pm 1.0) \times 10^{-6}$, $(7.7 \pm 2.5) \times 10^{-6}$, and $(1.1 \pm 0.2) \times 10^{-5}$, respectively. Sodalite-3 yields the highest inferred $(^{36}Cl/^{35}Cl)_o$ value, although the data show large scatter, probably indicating later disturbance in this grain. Therefore, the two assemblages with the highest Cl/S ratios (Fig. 2 *b* and *d*) yield the best determination of the inferred $(^{36}Cl/^{35}Cl)_o$ ratios of $\approx 5 \times 10^{-6}$ in the sodalite. The alteration assemblages in the two CAIs from the enstatite chondrites show no resolvable ^{36}S excess because of their low $^{35}Cl/^{34}S$ ratios (<100). Secondary ion images revealed the presence of very fine-grained hot spots of ^{34}S, suggesting the presence of tiny sulfides, which would mask any evidence of ^{36}Cl.

Analyses of the unaltered melilite/spinel-rich crust of the Ningqiang CAI show clear ^{26}Mg excesses that linearly correlate with the $^{27}Al/^{24}Mg$ values of the minerals (Fig. 3*a*), indicating *in situ* decay of ^{26}Al. The inferred $(^{26}Al/^{27}Al)_o$ ratio ($\pm 2\ \sigma$) is $(5.1 \pm 1.4) \times 10^{-5}$, consistent with previous observations in Ningqiang CAIs (18) and identical to the canonical $(^{26}Al/^{27}Al)_o$ value (5×10^{-5}) (19). However, neither anorthite nor the sodalite-rich assemblages in the CAI mantle show resolvable ^{26}Mg excess, providing a maximum inferred $(^{26}Al/^{27}Al)_o$ ratio of $\approx 0.7 \times 10^{-5}$ (Fig. 3*b*). Assuming the $(^{26}Al/^{27}Al)_o$ ratios of melilite and sodalite reflect a temporal difference, then sodalite formed ≥2 My after the formation of melilite.

Discussion

Because of the high Cl concentration of sodalite, ^{36}Cl may be cosmogenically produced by reaction of $^{35}Cl(n,\gamma)^{36}Cl$ during cosmic-ray exposure of the meteorite. However, the cosmogenic ^{36}Cl can be ignored according to the noble gas isotopic data. If there had been cosmogenic ^{36}Cl, we would have an excess of ^{36}Ar from its decay. This excess would increase the $^{36}Ar/^{38}Ar$ ratio that is used to calculate cosmogenic ^{38}Ar concentration. An increase in $^{36}Ar/^{38}Ar$ ratio causes the cosmogenic ^{38}Ar to be too low if we use a trapped $^{36}Ar/^{38}Ar$ ratio of 5.32. That means the cosmic-ray exposure (CRE) age calculated from cosmogenic ^{38}Ar will be lower than that from ^{3}He and ^{21}Ne. However, this is not the case: the CRE ages of the Ningqiang meteorite based on ^{36}Ar, ^{3}He, and ^{21}Ne are 43.5 ± 5.3, 43.4 ± 5.4, and 39.6 ± 4.0 My, respectively (20). Similarly, the estimated cosmogenic ^{36}Ar component decayed from the cosmogenic ^{36}Cl in the Efremovka matrix is also very low, <3% of the excess ^{36}Ar from decay of short-lived ^{36}Cl (15).

The inferred $(^{36}Cl/^{35}Cl)_o$ ratios of (5–11) $\times 10^{-6}$ for the Ningqiang CAI alteration assemblages are four to eight times higher than a previous estimate $(1.4 \pm 0.2) \times 10^{-6}$, which was derived from measurements of ^{36}Ar excess in the matrix of Efremovka (15). There are several possible explanations for the difference. First, the vast majority (94–96%) of ^{36}Ar in meteorites is a mixture of a trapped component, a spallation component, and the decay of cosmogenic ^{36}Cl. Estimation of ^{36}Ar excess from the decay of short-lived ^{36}Cl hence highly depends on accurate determination and subtraction of these components. A recent study of isotopic compositions of noble gases in meteorites showed a large variation of $^{38}Ar/^{36}Ar$ ratios caused by experimental artifact, requiring reassessment for the entire reported ^{36}Ar excess (21). Thus, it is likely that the previous report of ^{36}Cl decay products was inaccurate.

Second, the difference may be related to partial loss of gaseous ^{36}Ar during mild thermal metamorphism in the asteroidal body. The partial loss of ^{36}Ar in Ningqiang would be consistent with its significantly lower gas retention ages (^{40}K-^{40}Ar age of 4,260 ± 70 My and U/Th-^{4}He age of 4,170 ± 160 My, in comparison with the chondrite formation age of ≈4,560 My) (20). Although Efremovka may have a different parent body from that of Ningqiang, it probably lost some ^{36}Ar as well, because both meteorites are carbonaceous chondrites and experienced comparable mild thermal metamorphism (with the same petrographic type of 3) in their parent bodies. In contrast, little sulfur was lost during the same metamorphism event. Third, the different $^{36}Cl/^{35}Cl$ ratios of the Efremovka matrix and the Ningqiang sodalite may be caused by their distinct cosmic-ray exposure histories. However, as discussed above, the cosmogenic ^{36}Cl is negligible. Finally, it is possible that the difference may represent a time interval of 0.6–1.2 My (i.e., two to four times of the half-life of ^{36}Cl) between the alteration of the CAI and the formation of Efremovka matrix, with assumption of homogeneous distribution of ^{36}Cl in the nebula.

The inferred $(^{36}Cl/^{35}Cl)_o$ ratios of the sodalite cannot represent the initial value at the time when CAIs formed, because this Cl-rich mineral is an alteration product of the CAI (22). To deduce the initial $(^{36}Cl/^{35}Cl)_o$ value when the CAI

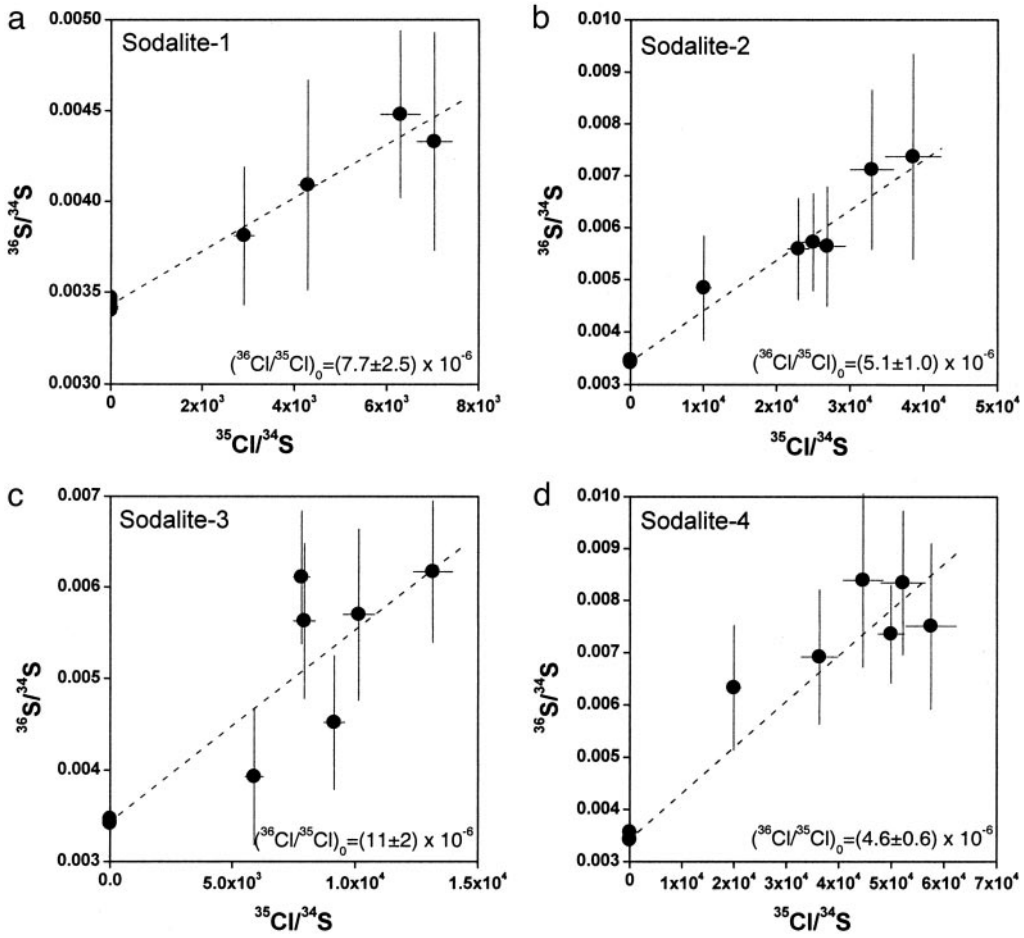

Fig. 2. Sulfur isotopic compositions of four sodalite-rich assemblages of the CAI (NQJ1-1#1) from the Ningqiang meteorite. All four analyses show clear excess of ^{36}S that linearly correlates with the Cl/S ratio, indicating *in situ* decay of ^{36}Cl in the assemblages. Error bars are 2 σ. The inferred $(^{36}Cl/^{35}Cl)_o$ ratios of the assemblages at the time of alteration are determined from the slopes of the best-fit correlation lines and are calibrated in proportion to the decay of ^{36}Cl to ^{36}S.

first formed, the time interval between the formation and alteration of the Ningqiang CAI is required. Such a time interval $\geq$2 My was determined based on the canonical $(^{26}Al/^{27}Al)_o$ ratio and the maximum inferred $(^{26}Al/^{27}Al)_o$ ratio of the anorthite and sodalite-rich assemblages. However, the lack of ^{26}Mg excesses in the anorthite and the sodalite-rich

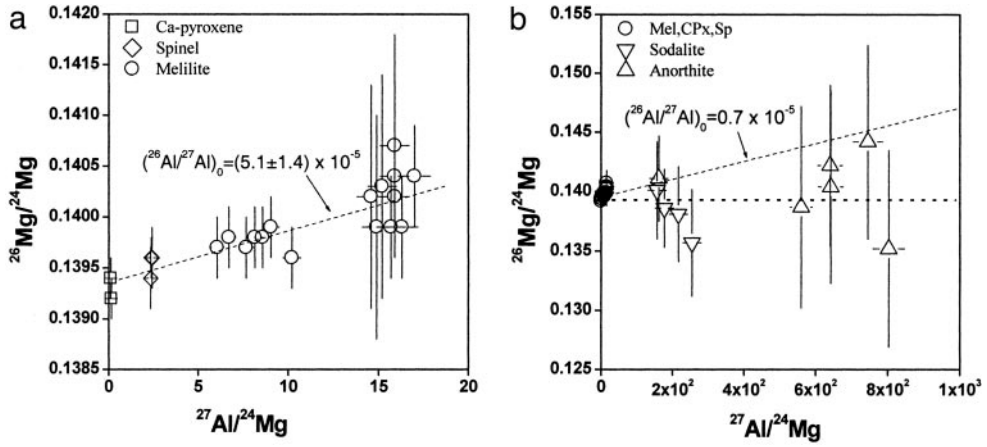

Fig. 3. Mg isotopic compositions and Al/Mg ratios of the same CAI. (*a*) Melilite in the unaltered crust of the inclusion shows clear ^{26}Mg excess that correlates with the Al/Mg ratios. Spinel and Ca-pyroxene occur in the crust. The inferred $(^{26}Al/^{27}Al)_o$ ratio is determined from the slope of the best-fit line of the analyses. Error bars are 2 σ. (*b*) Anorthite and the sodalite-rich alteration assemblage show no significant ^{26}Mg excess. The dashed line refers to a $(^{26}Al/^{27}Al)_o$ ratio of 0.7×10^{-5}, the upper limit; the dot horizontal line refers to the normal $^{26}Mg/^{24}Mg$ ratio of 0.139. Error bars are 2 σ. The analysis data are given in Table 2, which is published as supporting information on the PNAS web site.

assemblages may be partially caused by metamorphism that occurred much later on the parent body of Ningqiang. The ^{26}Al-^{26}Mg systematics of plagioclase in a plagioclase- and fassaite[‡‡]-rich (type C) inclusion and plagioclase- and olivine-rich inclusions from the same meteorite also show little ^{26}Mg excess (23). In accordance with self-diffusion rates of Mg in anorthite, it takes <2 My to homogenize Mg isotopes of the anorthite layers (<10 μm, in width) in the CAI at 500°C (23). Therefore, the $(^{26}Al/^{27}Al)_o$ ratios in anorthite or sodalite might reflect redistribution of Mg isotopes during metamorphism on the parent body. However, the ^{36}Cl-^{36}S system may not be significantly disturbed by the same event, because there are no S-bearing minerals surrounding the sodalite-rich assemblages. Assuming NQJ1-1#1 was an unmelted CAI that endured the same heating event that produced type C inclusions (22), a time interval of 1.5 My between the formation of the unaltered crust of NQJ1-1#1 and the heating event can be estimated according to the canonical value and the maximum $(^{26}Al/^{27}Al)_o$ ratio of type C inclusions ($\approx 1 \times 10^{-5}$) (19, §§). The same time difference (1.5 My) can be referred to as the minimum interval between the formation and alteration of the Ningqiang CAI. Using this time difference and the best inferred $(^{36}Cl/^{35}Cl)_o$ value ($\approx 5 \times 10^{-6}$) of sodalite, the initial $(^{36}Cl/^{35}Cl)_o$ ratio at the time when CAIs formed is then deduced to be $\geq 1.6 \times 10^{-4}$.

The initial $(^{36}Cl/^{35}Cl)_o$ value can be used to constrain the source of short-lived radionuclides and the setting of solar system formation. Wasserburg *et al.* (3) assumed that the solar system formation was triggered by explosion of a nearby supernova, and ^{36}Cl and other short-lived radionuclides were injected into the protosolar nebula. The predicted initial $(^{36}Cl/^{35}Cl)_o$ ratios of the solar nebula range from 3×10^{-6} to 2×10^{-4} (3), with consideration of a dilution factor for the supernova material to force a canonical $(^{26}Al/^{27}Al)_o$ ratio and by using the yields of massive stars reported in ref. 24. The predictions are consistent with the initial $(^{36}Cl/^{35}Cl)_o$ ratio of $\geq 1.6 \times 10^{-4}$ estimated in this study. Recent calculations report somewhat higher yields of ^{36}Cl/^{35}Cl relating to ^{26}Al/^{27}Al for massive stars (25). The new data may enhance the initial $(^{36}Cl/^{35}Cl)_o$ values, but are still consistent with our observations. On the other hand, ^{36}Cl might be synthesized in a nearby low-mass asymptotic giant branch star instead of a supernova. However, a low-mass asymptotic giant branch star source predicted much lower initial $(^{36}Cl/^{35}Cl)_o$ ratios ($\leq 7.85 \times 10^{-7}$ to 2.4×10^{-6}) (5, 6).

Alternatively, local irradiation models predict an upper limit of $(^{36}Cl/^{35}Cl)_o = 1.3 \times 10^{-4}$ (4). Although the predicted value is consistent with the observation from this study, the volatile nature of chlorine and the observation of ^{36}Cl in sodalite probably are not compatible with local irradiation models. According to the model by Shu *et al.* (10, 11), intense irradiation of the proto-sun evaporated Mg-Fe-silicate dust balls to form CAIs and simultaneously produced short-lived radionuclides (e.g., ^{10}Be, ^{26}Al, and ^{41}Ca) through the bombardment of CAI materials by energetic particles. After their formation, short-lived radionuclides bearing CAIs were ejected to distant locations where chondrites accreted. Sodalite, a volatile-rich (Na and Cl) alteration product, could not form together with the CAI primary minerals during the intense irradiation near the proto-sun. Instead, it almost certainly formed in the chondrite-accreting locations in the nebula and/or the asteroidal bodies. Therefore, in the local irradiation model, ^{36}Cl itself would have to be produced in a gaseous phase close to the proto-sun by intense irradiation, and then a mechanism to transport the gaseous ^{36}Cl, coupled with solids, from the CAI-forming region to distant chondrite-accreting regions must be invoked. Finally, the transported gaseous ^{36}Cl would have to be incorporated into alteration assemblages through solid-gas reaction. However, the transported gaseous ^{36}Cl must have been much diluted before it was incorporated into the alteration assemblages. Furthermore, according to the local irradiation model (10), gases and small particles would be thrown into interstellar space with finite escape speeds, decoupled from the large CAIs that fell back to the disk. Therefore, the observation of ^{36}Cl in this study presents a serious challenge to local irradiation models.

CAIs and chondrules in carbonaceous chondrites are commonly altered to produce sodalite and other secondary minerals (17). However, where the alteration took place, in the nebula or the asteroidal bodies, is a highly controversial issue. One approach is to determine ages of sodalite and other alteration products. The I-Xe (half-life of ^{129}I, 15.7 My) data of Allende sodalite-rich samples suggest an apparent closure time of 5 My after Murchison magnetite (26), marginally longer that the predicted lifetime of the solar nebula. However, the long closure age may be caused by partial loss of gaseous ^{129}Xe during thermal metamorphism in the parent body. Other data on Al-Mg systems of sodalite suggest the time intervals of several My after formation of CAI primary minerals (19, §§, ¶¶), but they also may be explained by diffusion of normal Mg isotopes from common surrounding Mg-rich phases as discussed above. ^{36}Cl has a shorter half-life than those of ^{26}Al and ^{129}I, and discovery of the short-lived ^{36}Cl in sodalite favors for a short interval (e.g., a few half-lives of ^{36}Cl), otherwise it would have decayed and little can be detected. This short time interval favors a nebular origin of sodalite in the Ningqiang CAI, consistent with petrography and mineral chemistry (22).

Conclusions

Sodalite-rich alteration assemblages in a Ningqiang CAI show clear excess of ^{36}S that linearly correlates with Cl/S ratios of the assemblages, providing direct evidence for the presence of short-lived ^{36}Cl in the early solar system. The best inferred $(^{36}Cl/^{35}Cl)_o$ ratio of sodalite is 5×10^{-6}. Combined with the ^{26}Al-^{26}Mg systems of the individual minerals and petrographic settings of the CAI, the initial $(^{36}Cl/^{35}Cl)_o$ ratio of the solar nebula is determined to be $\geq 1.6 \times 10^{-4}$.

The presence of ^{36}Cl in the sodalite-rich alteration assemblages of the Ningqiang CAI and the initial $(^{36}Cl/^{35}Cl)_o$ ratio are consistent with a supernova source of short-lived radionuclides, whereas a low-mass asymptotic giant branch star source predicts a much lower $(^{36}Cl/^{35}Cl)_o$ ratio. Although ^{36}Cl can be produced by local irradiation of the proto-sun, its volatile nature and occurrence in alteration assemblages of CAIs present a serious challenge for local irradiation models.

Unlike other short-lived radionuclides (e.g., ^{26}Al and ^{41}Ca), chlorine is closely associated with secondary alteration in CAIs, chondrules, and matrix. ^{36}Cl may serve as a unique fine-scale chronometer, especially for volatile-rock reactions in the nebula and/or on asteroidal bodies. The discovery of ^{36}Cl in sodalite favors a short time interval after formation of CAI primary minerals, consistent with a nebular origin of the alteration in the Ningqiang CAI.

[‡‡]Ti- and Al-rich Ca-pyroxine.

[§§]Kita, N. T., Lin, Y., Kimura, M. & Morishita, Y. (2004) *Lunar Planet. Sci.* **35,** 1471 (abstr.).

[¶¶]Hutcheon, I. D. & Newton, R. C. (1981) *Lunar Planet. Sci.* **XII,** 491–493 (abstr.).

We thank G. Huss and O. Eugster for helpful discussion. This article was significantly improved by constructive reviews by K. D. McKeegan and L. R. Nittler. This study was supported by National Natural Science Foundation of China to Grants 40232026 and 40025311 (to Y.L.) and the National Aeronautics and Space Administration (L.A.L.).

1. Zinner, E. (2003) *Science* **300,** 265–267.
2. Gilmour, J. (2002) *Science* **297,** 1658–1659.
3. Wasserburg, G. J., Gallino, R. & Busso, M. (1998) *Astrophys. J.* **500,** L189–L193.
4. Leya, I., Halliday, A. N. & Wieler, R. (2003) *Astrophys. J.* **594,** 605–616.
5. Gallino, R., Busso, M., Wasserburg, G. J. & Straniero, O. (2004) *New Astron. Rev.* **48,** 133–138.
6. Busso, M., Gallino, R. & Wasserburg, G. J. (1999) *Annu. Rev. Astron. Astrophys.* **37,** 239–309.
7. Cameron, A. G. W. (1995) *Meteoritics* **30,** 133–161.
8. Amelin, Y., Krot, A. N., Hutcheon, I. D. & Ulyanov, A. A. (2002) *Science* **297,** 1678–1683.
9. Bizzarro, M., Baker, J. A. & Haack, H. (2004) *Nature* **431,** 275–278.
10. Shu, F. H., Shang, H. & Lee, T. (1996) *Science* **271,** 1545–1552.
11. Shu, F. H., Shang, H., Glassgold, A. E. & Lee, T. (1997) *Science* **277,** 1475–1479.
12. Lee, T., Shu, F. H., Shang, H., Glassgold, A. E. & Rehm, K. E. (1998) *Astrophys. J.* **506,** 898–912.
13. Gounelle, M., Shu, F. H., Shang, H., Glassgold, A. E., Rehm, K. E. & Lee, T. (2001) *Astrophys. J.* **548,** 1051–1070.
14. Endt, P. M. (1990) *Nuclear Physics* **521,** 1–400.
15. Murty, S. V. S., Goswami, J. N. & Shukolyukov, Y. A. (1997) *Astrophys. J.* **475,** L65–L68.
16. Grossman, L. (1972) *Geochim. Cosmochim. Acta* **36,** 597–619.
17. MacPherson, G. J., Wark, D. A. & Armstrong, J. T. (1988) in *Meteorites and the Early Solar System*, eds. Kerridge, J. F. & Matthews, M. S. (Univ. Arizona Press, Tucson), pp. 746–807.
18. Hsu, W., Huss, G. R. & Wasserburg, G. J. (2003) *Meteorit. Planet. Sci.* **38,** 35–48.
19. MacPherson, G. J., Davis, A. M. & Zinner, E. (1995) *Meteoritics* **30,** 365–386.
20. Eugster, O., Michel, T. & Niedermann, S. (1988) *Meteoritics* **23,** 25–27.
21. Rai, V. K., Murty, S. V. S. & Ott, U. (2003) *Geochim. Cosmochim. Acta* **67,** 4435–4456.
22. Lin, Y. & Kimura, M. (1998) *Meteorit. Planet. Sci.* **33,** 435–446.
23. LaTourrette, T. & Wasserburg, G. J. (1998) *Earth Planet. Sci. Lett.* **158,** 91–108.
24. Woosley, S. E. & Weaver, T. A. (1995) *Astrophys. J.*, Suppl. **101,** 181–235.
25. Rauscher, T., Heger, A., Hoffman, R. D. & Woosley, S. E. (2002) *Astrophys. J.* **576,** 323–348.
26. Swindle, T. D. (1998) *Meteorit. Planet. Sci.* **33,** 1147–1155.